Am J Cancer Res 2022;12(10):4680-4692
www.ajcr.us /ISSN:2156-6976/ajcr0138041

Original Article

Inhibition of EP2 receptor suppresses tumor growth and chemoresistance of gastric cancer

Vivian Yvonne Shin*, Michelle Xin Liu*, Jennifer Man-Ting Siu, Ava Kwong, Kent-Man Chu

*Department of Surgery, The University of Hong Kong, Hong Kong SAR 999077, China. *Equal contributors.*

Received August 5, 2021; Accepted July 20, 2022; Epub October 15, 2022; Published October 30, 2022

Abstract: Gastric cancer is one of the leading causes of cancer death in the world. Early diagnosis and effective chemotherapy are vital to reduce the overall mortality. Prostaglandin E2 (PGE2) has been implicated as an important factor in gastric cancer carcinogenesis. ECF based regimen (epirubicin, cisplatin, 5-fluorouracil) is the first-line chemotherapy for advanced gastric cancer. However, patients develop resistance after chemotherapy. The aim of this study is sought to investigate the role of EP2 receptor, a PGE_2 receptor, and the antagonism of EP2 receptor in response to ECF treatment. Expression of EP2 receptor was evaluated in gastric cancer tissue samples and cell lines. Cell proliferation and cell apoptosis assays were performed *in vitro* and *in vivo,* upon knockdown of EP2 receptor, antagonist of EP2 receptor and/or ECF treatment. Western Blot was applied for evaluation of proteins relating to cell cycle, apoptosis and drug transporter. Next generation sequencing and ingenuity pathway analysis were applied for screening for downstream targets of EP2 receptor. Expressions of the targets of EP2 receptor were further evaluated in gastric cancer cells and tissues. In this study, we found that expression of EP2 receptor was significantly upregulated in gastric cancer. Inhibition of EP2 receptor reduced gastric cancer cell proliferation, induced cell cycle arrest proteins, and enhanced cell apoptosis. Moreover, knockdown of EP2 receptor by siRNA or antagonist sensitized gastric cancer cells to ECF. Silence of EP2 receptor also significantly abrogated gastric cancer growth in a mice model. Analysis revealed that CAV1 was a downstream target of EP2 receptor in gastric cancer. Our findings illustrated that blocking EP2 receptor reduced tumor growth and induced apoptosis in gastric cancer. This novel study unraveled CAV1 was a downstream target of EP2 receptor. Antagonizing EP2 receptor could be a potential therapeutic target in gastric cancer, in particular those with high EP2 receptor expression.

Keywords: EP2 receptor, proliferation, apoptosis, chemoresistance, gastric cancer

Introduction

Gastric cancer is one of the leading causes of cancer death in the world [1]. Around 70% of the gastric cancer cases occur in Eastern Asia, with the highest morbidity in China, Korea and Japan [2]. Surgery remains the mainstay for curative treatment for gastric cancer. However, more than 60% of the tumors are unresectable when diagnosed. Systemic chemotherapy is, therefore, given to patients with advanced disease, where ECF based regimen (epirubicin, cisplatin, 5-fluorouracil) is commonly used for these patients. The efficacy of chemotherapy was unobtrusive due to development of chemoresistance, resulting in tumor recurrence and metastasis.

Enormous evidence reported that expression of COX-2 was upregulated in many cancers and was shown to promote angiogenesis and tumor growth [3-5]. Inhibitors of COX-2 were reported to exert tumor suppressive effects and enhance chemosensitivity to anti-cancer drug by abrogation of prostaglandins synthesis, in particular prostaglandin E_2 (PGE_2) [6-8]. Despite the promising effects of COX-2 inhibitors, the unwanted side effects, in particular, cardiovascular risk cannot be ignored. Studies have extended to explore the downstream receptors of prostanoid, hoping to improve drug sensitivity with minimal side effects.

Prostanoids exerted biological effects through activation of G protein coupled receptors, such as E-type prostanoid receptors (EP) [9]. There are four G-protein-coupled cell surface receptor subtypes of EP receptors, including EP1, EP2, EP3 and EP4. The binding of these receptors to ligands elicits different signaling pathways and

cellular functions. A number of studies have indicated EP receptors play important roles in cancer development and progression [10-12]. Our previous study also demonstrated that blocking EP2 or EP4 receptors suppressed gastric cancer growth and angiogenesis through p38 phosphorylation [13, 14]. These studies implicated that EP receptor contributed to gastric cancer growth, however, the detailed signaling pathways has not been explored.

In our preliminary study, we demonstrated that overexpression of EP2 receptor was seen in gastric cancer tissue samples than other EP receptor subtypes by RT-qPCR. Therefore, we aim to evaluate the role of EP2 receptor in the growth of gastric cancer and its contribution to chemoresistance in gastric cancer. We also identified a crucial downstream target of EP2 receptor to elucidate the molecular mechanism in gastric carcinogenesis.

Materials and methods

Human tissue samples

Paired human gastric cancer tissues and non-tumor tissues (N = 32 pairs) (Stage I, N = 10; Stage II, N = 8; Stage III, N = 6; Stage IV, N = 8) were collected in Queen Mary Hospital, Hong Kong. Tumor tissues were confirmed to be malignant by experienced pathologist. Informed consent were obtained from all the patients. None of the participants received pre-operative therapy. The samples were frozen in liquid nitrogen and stored at -70°C.

Gastric cancer cell lines

Human gastric cancer cells, AGS (ATCC, Rockville, MD, USA) and MKN45 (Riken, Japan), were used in this study. Cells were cultured in RPMI-1640 medium (Gibco BRL, Gaithersburg, MD, USA) supplemented with 10% fetal bovine serum (Gibco BRL). All cells were incubated in a humidified incubator with 5% CO_2 at 37°C.

RNA extraction and RT-qPCR

Around 20 mg of tissue sample or 10^6 cell pellet were used for RNA extraction using RNeasy Mini Kit (Qiagen, Hilden, Germany) following the manufacturer's instructions. The concentrations of RNA samples were quantified by NanoDrop 1000 (Nanodrop, Wilmington, Delaware, USA). 500 ng of total RNA from each sample were subjected to reverse transcription (RT).

Briefly, RNA (500 ng) from tissues or cells were reverse transcribed to cDNA using Omniscript RT Kit (Qiagen, Hilden, Germany). Real-time RT-PCR (RT-qPCR) was performed using SYBR Green PCR Kit (Qiagen) in ABI ViiA7 real-time PCR system (Applied Biosystems, Waltham, MA, USA). The mRNA expression was normalized to actin or GAPDH. Fold change in the gene was calculated by the equation $2^{-\Delta\Delta Ct}$. Specific primers of the genes were summarized in Supplementary Table 1.

MTT assay

Briefly, 5000 cells/well were seeded in 96-well plates and transfected with control siRNA or EP2 receptor siRNA (SI02757580, Qiagen) or EP2 receptor antagonist (AH6809, 3 μM) using Lipofectamine 3000 (Invitrogen, Waltham, USA) for 3 days and incubated with or without ECF (1 μM epirubicin, 4 μM cisplatin and 20 μM 5-fluorouracil). After 48 hours, 3% MTT solution were incubated for 3 hours. Finally, dimethyl sulfoxide (DMSO, Sigma-Aldrich) was added for 30 minutes and the absorbance (570 nm) was measured by Multiskan™ FC Microplate Photometer (Thermo Fisher Scientific, Waltham, USA). The assay was performed in triplicates and the result was showed as mean ± SD.

Apoptosis multi-target sandwich ELISA kit assay

Cells transfected with control siRNA or EP2 receptor siRNA (SI02757580, Qiagen) for 3 days and incubated with or without ECF. After treatment, cell lysates were used to detect apoptosis by PathScan® Apoptosis Multi-Target Sandwich ELISA Kit (Cell Signaling, Danvers, USA). Briefly, cell lysates were sonicated and centrifuged for 10 min at 4°C. After incubation with cell lysates overnight at 4°C, antibodies of p53, phospho-p53 (Ser15), Bad, phospho-Bad (Ser112), cleaved caspase-3 (Asp175) and cleaved PARP (Asp214) were incubated for 1 hour at 37°C. HRP-linked secondary antibody was then incubated for another 30 min at 37°C. TMB substrate was added and the absorbance was measured at 450 nm. The assay was performed in triplicated and the result was showed as mean ± SD.

Western blot analysis

Western Blot was performed for evaluation of protein expression of EP2 receptor and associated proteins in the samples. Protein was extracted with RIPA Buffer (Sigma Chemical Co., St Louis, MD, USA). Samples were resolved by SDS-PAGE and electroblotted onto Immobilon-P Transfer Membrane (Applied Biosystems). The membrane was blotted with antibody specific for anti-EP2 receptor (Cayman Chemical), anti-cyclin D3 (Cell Signaling Technology) and anti-p27 (Cell Signaling Technology), anti-ATP7A (Novus Biologicals, CO, USA), anti-ATP7B (Novus Biologicals), anti-CTR1 (Novus Biologicals) or anti-β-actin (Cell Signaling Technology), respectively. The membranes were incubated with secondary antibody conjugated to horseradish peroxidase (Amersham Pharmacia, Cleveland, OH). The membranes were developed by enhanced chemiluminescence (ECL) and exposed to X-ray film (FUJI photo Film, Tokyo, Japan).

Next generation sequencing (NGS)

MKN45 cells transfected with control or EP2 receptor siRNA (SI02757580, Qiagen) were subjected to NGS. Total RNA (5 μg) isolated from cell lines were used for NGS. The rRNA-depleted RNA sequencing was conducted on an Illumina HiSeq 1500 at the Centre of Pano-Omics Science of the University of Hong Kong. Sequencing raw reads were filtered for adapter sequence and low quality sequence, and retained reads with read length ≥40 bp. After that, sequencing reads were filtered for rRNA sequence and the remaining reads were subjected to downstream analysis. RSEM Version 1.2.21 was used for alignment, quantification and identification of differentially expressed genes (DEG). EBSeq Version 1.6.0 was used for the identification of DEG. The quality and analysis of the sequencing data was monitored by the bioinformatics team associated with the sequencing core.

Ingenuity pathway analysis (IPA)

A list of dysregulated genes with knockdown of EP2 receptor was generated from NGS. Interaction and correlation of these genes were analyzed with application of IPA (Qiagen). IPA is a web-based software application. It enables analysis, integration, and understanding of data from miRNA, gene expression, and SNP microarrays, as well as RNAseq experiments, proteomics and metabolomics. It provides identification of upstream regulators, insight into molecular interactions and cellular phenotypes, and discoveries about disease processes. It also provides information on target genes, and building of interactive models of experimental systems. Data analysis and search capabilities are beneficial in understanding the significance of data, specific targets or candidate biomarkers. This software is backed up by the Ingenuity Knowledge Base of highly structured, detail-rich biological and chemical findings.

Tumor growth in mice model

Athymic BALB/c-Nu/nu male nude mice, 6 weeks old, were implanted with MKN45 cells to act as human gastric cancer xenograft model. Briefly, 1×10^6 cells suspended in 100 μl PBS were inoculated subcutaneously into the right flank of the mice. They were randomly divided into two groups: scrambled control and EP2 receptor siRNA (N = 7 for each group). When the volume of the tumor had reached ~100 mm^3 (~7 days), EP2 receptor siRNA or control siRNA were mixed with Invivofectamine (Thermo Fisher Scientific, Waltham, USA) and administered subcutaneously around the tumor every 7 days for 4 weeks. The size of tumor was measured every 7 days, beginning from Day 7, and the tumor volume was calculated by $V = L \times W^2/2$ (where L = the largest dimension, W = perpendicular diameter). The relative tumor volume was represented as the average ratio of tumor volume at the time of measurement to the initial volume on Day 7 of each group.

Statistical analysis

Statistical analyses were carried out using Statistical Package for Social Sciences (SPSS) 24.0 for Windows (SPSS Inc., Chicago, IL, USA). Wilcoxon signed rank test was applied to analyze EP2 receptor expression in gastric cancer. Student's t test was used to analyze the results expressed as mean ± SD. All P-values are two-sided and a value of $P \leq 0.05$ is considered statistically significant.

Results

Expressions of EP receptors in gastric cancer tissues

To identify the specific EP receptors that contributed to gastric cancer development, 32

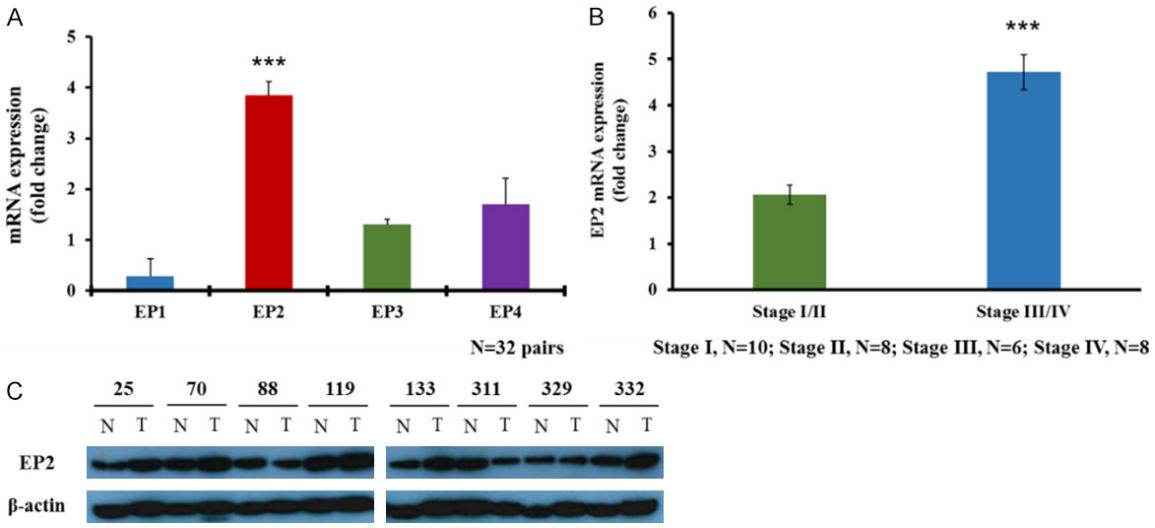

Figure 1. Expression of EP2 receptor in gastric cancer tissue samples. A. Expressions of EP1, EP2, EP3, and EP4 receptors in 32 pairs of gastric tumor and adjacent non-tumor tissues. Fold change represented the average ratio of expression in gastric tumor tissues to expression in non-tumor tissues of each EP receptor subtype. Expression of EP2 receptor was significantly higher in tumors than other EP receptor subtypes (N = 32 pairs, ***P<0.001). B. Expression of EP2 receptor was significantly increased in patients with Stage III and IV (Stage I, N = 10 pairs; Stage II, N = 8 pairs; Stage III, N = 6 pairs; Stage IV, N = 8 pairs; ***P<0.001). C. Representative of protein expression of EP2 receptor in paired gastric cancer tissues by Western Blot (N: adjacent non-tumor tissue; T: gastric cancer tissue).

pairs of gastric tumors and adjacent non-tumor tissues were analyzed by real-time PCR. Among all, EP2 receptor expression was markedly higher in tumors than other EP receptor subtypes (**Figure 1A**, ***P<0.001, N = 32 pairs). There was an association of EP2 receptor expression with tumor stage, increased expression of EP2 receptor was seen in patients with stage III and IV tumors (**Figure 1B**, ***P<0.001, Stage I, N = 10; Stage II, N = 8; Stage III, N = 6; Stage IV, N = 8). Moreover, evaluation of protein expression of EP2 receptor by Western Blot showed that EP2 was higher expressed in gastric cancer tissues compared with non-tumor tissues (**Figure 1C**). Therefore, EP2 receptor was selected for further study.

Role of EP2 receptor in gastric cancer growth

Cells transfected with EP2 receptor siRNA caused reduction in cell proliferation in AGS and MKN45. ECF is the first-line chemotherapy regimen for treating gastric cancer patients. Combining treatment with ECF and EP2 receptor siRNA has more prominent effect on inhibiting cell proliferation when compared with siRNA alone group (**Figure 2A**, **P<0.01, ***P<0.001). Similarly, combining EP2 receptor antagonist AH6809 and ECF repressed cell proliferation to a greater extent than ECF alone (**Figure 2B**, **P<0.01, ***P<0.001). This indicated that blockade of EP2 receptor sensitized cells to ECF treatment. Similarly, reduced expression of EP2 receptor inhibited the colony formation ability of AGS and MKN45 cells (**Figure 2C**, ***P<0.001). Western Blot analysis showed that silence of EP2 receptor reduced cell cycle proteins including Cyclin D3 and p27 in AGS and MKN45 cells (**Figure 2D**). It suggested that inhibition of EP2 receptor induced cell cycle arrest.

Blocking EP2 receptor induced apoptosis

To examine the effect of EP2 receptor on apoptosis, PathScan® Apoptosis Multi-Target Sandwich ELISA was used to evaluate apoptosis in cells treated with EP2 receptor siRNA. Treatment with siRNA increased the proportion of apoptosis, and combination with ECF further increased apoptosis (**Figure 3A**, **P<0.01, ***P<0.001). The proteins that involved in apoptosis were assessed by Western Blot. Increased cleaved caspase-3 and decreased Bcl2 expressions were further induced in cells with EP2 receptor siRNA and ECF treatment (**Figure 3B**).

Antagonism of EP2 receptor enhanced chemosensitization

Cell proliferation of EP2 receptor siRNA plus ECF-treated cells were decreased more dra-

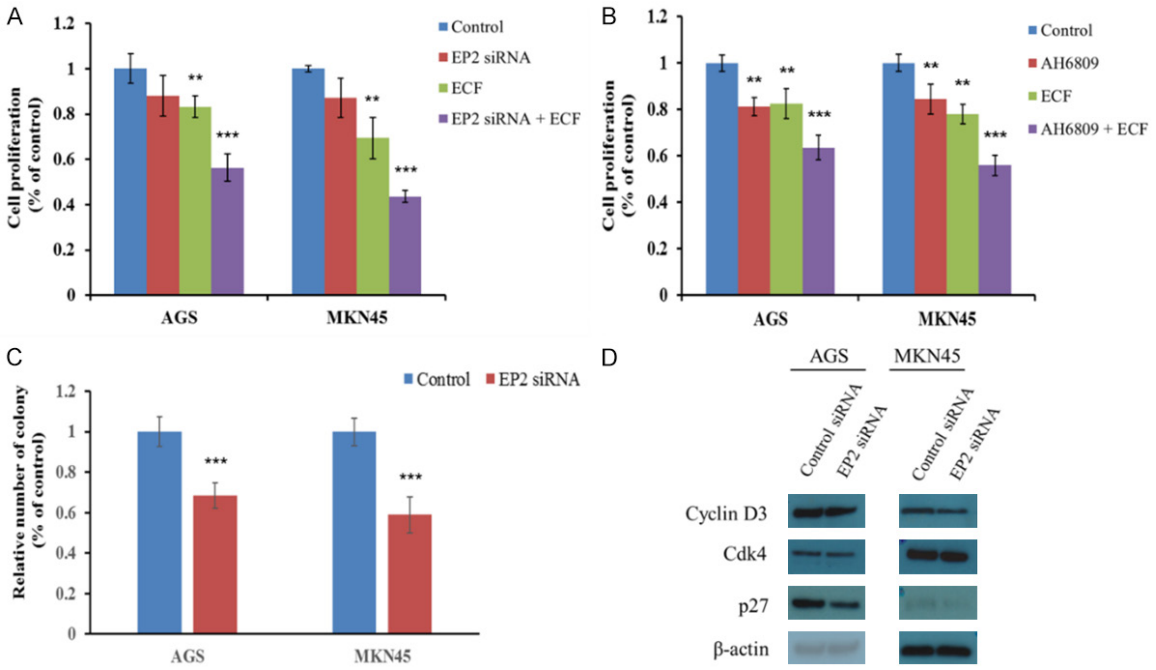

Figure 2. Functional roles of EP2 receptor in gastric cancer. A and B. Knockdown of EP2 receptor by siRNA or EP2 antagonist AH6809 (3 μM), with combination of ECF (1 μM epirubicin, 4 μM cisplatin and 20 μM 5-fluorouracil) for 48 hours, would significantly reduce cell proliferation in AGS and MKN45 cells (***P*<0.01, ****P*<0.001). C. Blockade of EP2 receptor by siRNA significantly inhibited the colony formation ability of AGS and MKN45 cells (****P*<0.001). D. Western Blot analysis showed that EP2 receptor siRNA remarkably reduced cell cycle protein expressions of Cyclin D3 and p27 in AGS and MKN45 cells.

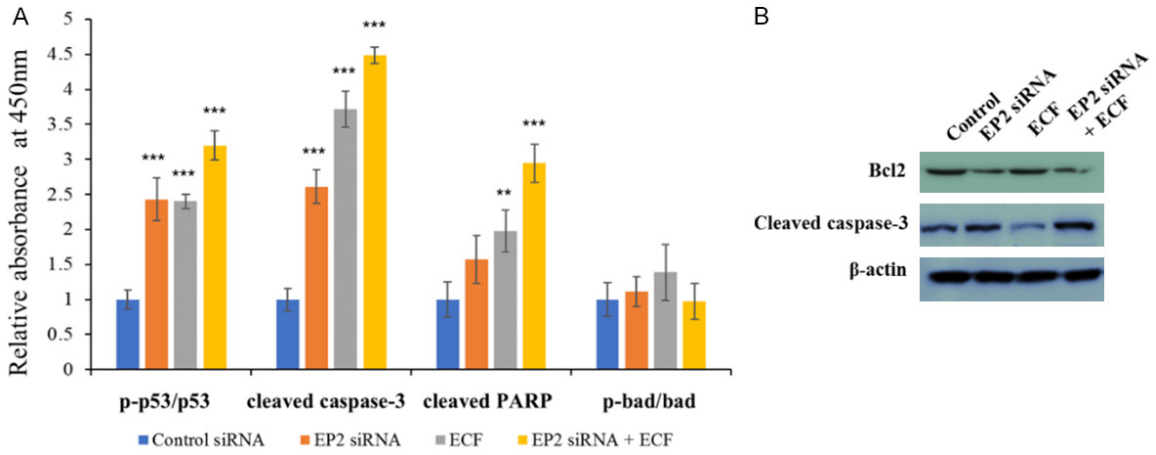

Figure 3. Blockage of EP2 receptor induced apoptosis. A. Apoptosis assay by ELISA in cells treated with EP2 receptor siRNA significantly increased the proportion of apoptosis including p-p53/p53, cleaved caspase-3, and cleaved PARP. Combination with EP2 receptor siRNA and ECF further increased apoptosis (***P*<0.01, ****P*<0.001). B. Increased cleaved caspase-3 and decreased Bcl2 expressions were induced in cells with combination of EP2 receptor siRNA and ECF as indicated by western blot. The result was showed as mean ± SD.

matically than EP2 receptor siRNA or AH6809 alone. We further revealed the molecular mechanism of EP2 receptor on chemosensitivity in gastric cancer. QPCR showed that expressions of ATP7A and ATP7B (copper-transporting P-type adenosine triphosphatase) were upregulated upon ECF treatment, while EP2 receptor siRNA plus ECF significantly reduced their expressions (**Figure 4A**, **4B**, ***P*<0.01, ****P*<0.001). In AGS, CTR1 (copper transporter 1)

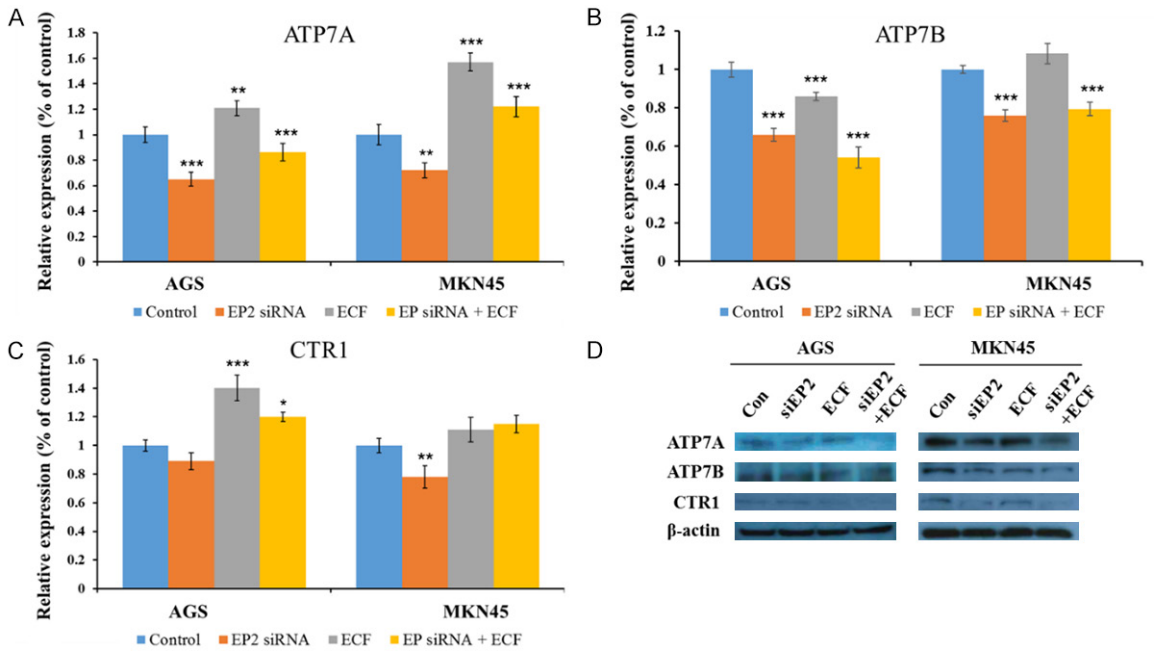

Figure 4. Expressions of ATP7A, ATP7B and CTR1 in gastric cancer cells. A and B. Expressions of ATP7A and ATP7B were upregulated upon ECF treatment, while EP2 receptor siRNA significantly reduced the expressions in AGS and MKN45 cells (***P*<0.01, ****P*<0.001). C. Expression of CTR1 was increased in AGS and MKN45 cells with ECF and combination of EP2 siRNA and ECF (**P*<0.05, ****P*<0.001). D. Western Blot analysis showed the protein expressions of ATP7A, ATP7B and CTR1 in different treatment groups including control group, siRNA EP2, ECF and siRNA EP2 plus ECF.

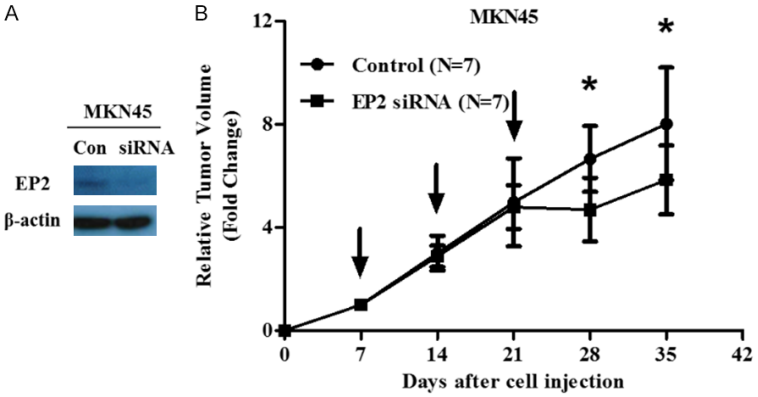

Figure 5. Knockdown of EP2 in tumor growth *in vivo*. A. Validation of knockdown of EP2 receptor in MKN45 cells by Western Blot. B. The tumor volumes were measured every 7 days for each group. The relative tumor volume represented the average ratio of tumor volume at the time of measurement to the initial volume on Day 7 of each group. The tumor volume was significantly smaller in mice with EP2 receptor siRNA than control starting from Day 28 (**P*<0.05). The arrows indicated the injection of control or EP2 receptor siRNA into the mice each week. The result was showed as mean of fold change ± SD.

was increased in cells with ECF and combination of EP2 receptor siRNA and ECF (**Figure 4C**, **P*<0.05, ***P*<0.01, ****P*<0.001). Protein expressions of ATP7A, ATP7B and CTR1 in different treatment groups were indicated in **Figure 4D**. These data suggested that EP2 receptor silencing enhanced the retention of ECF through regulation of drug transporter genes in cancer cells, which subsequently reduced cell proliferation.

Knockdown of EP2 receptor inhibited tumor growth in vivo

To examine the effect of knockdown of EP2 receptor on tumor growth, tumor volume of mice between control and EP2 receptor siRNA were compared. Knockdown of EP2 receptor by siRNA in gastric cancer cells MKN45 was validated by Western Blot (**Figure 5A**). Injection of EP2 receptor siRNA into the tumor was executed each week (indicated by the arrows on **Figure 5B**). The result showed that tumor volume was significantly smaller in mice with EP2 receptor siRNA

Table 1. Number of reads and differentially expressed genes of next generation sequencing

1	Lipid Metabolism, Molecular Transport, Small Molecule Biochemistry	47	24
2	Cellular Movement, Cell-To-Cell Signaling and Interaction, a Connective Tissue Development and Function	27	16
3	Cellular Assembly and Organization, Neurological Disease, Nucleic Acid Metabolism	22	14
4	Cell Death and Survival, Cell Cycle, Cellular Compromise	20	13
5	Cancer, Cell Death and Survival	20	14
6	Developmental Disorder, Glomerular Injury, Organismal Injury and Abnormalities	19	12
7	Immunological Disease, Inflammatory Disease, Respiratory Disease	19	12
8	Cellular Development, Organismal Development, Organismal Injury and Abnormalities	19	12
9	Tissue Morphology, Connective Tissue Disorders, Organismal Injury and Abnormalities	19	12
10	Protein Synthesis, Cell Death and Survival, Cellular Compromise	17	12
11	Cell Cycle, Cellular Growth and Proliferation, Connective Tissue Development and Function	17	11
12	Cancer, Gastrointestinal Disease, Hepatic System Disease	8	7
13	Cardiovascular Disease, Cardiovascular System Development and Function, Cell Morphology	2	1
14	Post-Translational Modification, Hereditary Disorder, Neurological Disease	2	1
15	RNA Post-Transcriptional Modification, Cancer, Organismal Injury and Abnormalities	2	1

Table 2. Networks of the dysregulated genes released from ingenuity pathway analysis

Sample	Number of Raw Reads	Number of Filtered Reads	Number of reads mapped to GRCh38	Number of Differentially Expressed Genes
MKN45-siControl	141,326,822	140,026,612	107,179,638	282
MKN45-siEP2	137,184,468	135,851,276	104,419,124	

than control siRNA (**Figure 5B**, **P*<0.05, N = 7 for each group), implicating knockdown of EP2 receptor significantly abrogated gastric cancer growth in the mice model.

Identification of downstream targets of EP2 receptor by next generation sequencing (NGS)

EP2 receptor was upregulated in gastric cancer and inhibition of EP2 receptor abrogated gastric cancer growth, downstream targets and associated pathways of EP2 receptor was further investigated. MKN45 cells transfected with control or EP2 receptor siRNA were subjected to NGS. The work flow of data analysis was summarized in Supplementary Figure 1. Filter of sequencing reads, reads mapped to the human transcriptome (GRCh38) and the total number of differentially expressed genes were summarized in **Table 1**. By comparing the expression profiles of MKN45-siControl and MKN45-siEP2, 281 genes with differential expressions were identified with false discovery rate FDR<0.05 (Supplementary Figure 2 and Supplementary Table 2). These dysregulated genes were potentially the downstream targets of EP2 receptor.

Analysis of targets of EP2 receptor with ingenuity pathway analysis (IPA)

The list of 281 dysregulated genes was subjected to online analysis with IPA. The result of IPA suggested that these genes were associated with 15 networks. Among these networks, five of them contributed to cancer development, including cellular movement (network 2), cell death and survival (network 4 and 5), cellular growth and proliferation (network 11), as well as cancer, gastrointestinal disease (network 12) (highlighted in **Table 2**). Dysregulated genes belong to the above five networks were summarized in **Table 3**. We showed that EP2 receptor contributed to gastric cancer growth and chemoresistance, it might exert its effects on the downstream targets associated with cellular movement (metastasis), cell survival and cellular proliferation. Taken account into the fold changes, *P*-values and literature review, six dysregulated genes ARRDC3, CAV1, GADD45A, DCBLD2, DCUN1D1 and NES were selected for further validation (**Table 4**).

Expressions of these six genes were evaluated in MKN45 cells by qPCR. Expression of CAV1

Table 3. Genes associated with networks

Network 2	Cellular Movement, Cell-To-Cell Signaling and Interaction, Connective Tissue Development and Function			
Gene name	chromosome	Fold Change	Regulation Type	*P*-value
DCBLD2	chr3	1.487044	Down	9.10E-14
DKK1	chr10	1.352854	Up	2.97E-08
PPM1L	chr3	1.340014	Down	5.23E-06
CPD	chr17	1.306877	Down	1.10E-05
ERRFI1	chr1	1.280873	Up	0.00015116
NES	chr1	1.321734	Down	0.00016649
PLAU	chr10	1.308931	Up	0.000383819
COL7A1	chr3	1.45531	Down	0.000769925
NCS1	chr9	1.323084	Down	0.001727821
GADD45A	chr1	1.267846	Up	0.006050188
NRP1	chr10	1.255486	Up	0.008614815
ACTA2	chr10	1.417433	Up	0.009238232
STK26	chrX	1.247588	Down	0.010705784
SLC7A7	chr14	1.291558	Down	0.025698983
Network 4	Cell Death and Survival, Cell Cycle, Cellular Compromise			
Gene name	chromosome	Fold Change	Regulation Type	*p*-value
ATP11C	chrX	1.445964	Down	2.97E-10
SH3BGRL2	chr6	1.403358	Down	8.53E-10
DENR	chr12	1.401552	Down	1.03E-09
RNASE4	chr14	1.331077	Down	0.000743747
ARL14	chr3	1.267646	Up	0.003339985
SERPINA3	chr14	1877.471	Up	0.003488631
LRRC58	chr3	1.253228	Down	0.006302783
AKAP2	chr9	1.898385	Down	0.018759159
ERN2	chr16	1.254233	Down	0.022714656
SH3D21	chr1	1.381422	Down	0.038048478
MEGF6	chr1	1.254133	Down	0.049494599
SNORA70	chrX	1.501935	Up	0.00215542
Network 5	Cancer, Cell Death and Survival			
Gene name	chromosome	Fold Change	Regulation Type	*p*-value
MPZL2	chr11	1.540662	Down	0
PTPRR	chr12	1.6791	Up	1.12E-10
PGM2L1	chr11	1.367704	Up	8.33E-08
VEGFA	chr6	1.306139	Down	1.49E-05
MGAT3	chr22	1.964225	Down	5.55E-05
EPS8L3	chr1	1.331531	Down	0.009230782
SEMA3B	chr3	1.309351	Down	0.010904548
TRIM2	chr4	1.240246	Down	0.012051141
MBNL1	chr3	1.239449	Up	0.012824855
IL31RA	chr5	1.602874	Up	0.024354936
NR1H3	chr11	1.285944	Down	0.035341401
INPP5D	chr2	1.448233	Up	0.042075734
PRRG4	chr11	1.265189	Down	0.042177567
Network 11	Cell Cycle, Cellular Growth and Proliferation, Connective Tissue Development and Function			
Gene name	chromosome	Fold Change	Regulation Type	*p*-value
CAV1	chr7	1.572301	Up	0
PABPC4	chr1	1.352475	Up	1.43E-07
DYNC1I1	chr7	1.715791	Up	0.00017995
CYP4F3	chr19	1.53462	Down	0.00040895
CDKN1A	chr6	1.283959	Up	0.000476092

GIPC2	chr1	1.281601	Down	0.005193539
RAB9A	chrX	1.301629	Down	0.018992839
RNU4-1	chr12	2.120475	Up	0
RNU2-1	chr17	1.473567	Up	1.70E-14
RNU6-1	chr15	1.954867	Up	1.30E-05
Network 12	Cancer, Gastrointestinal Disease, Hepatic System Disease			
Gene name	chromosome	Fold Change	Regulation Type	*p*-value
KLHL42	chr12	1.454888	Down	1.19E-11
MT-ND4	chrM	1.393679	Down	6.76E-06
DCUN1D1	chr3	1.309115	Down	6.19E-05
MT-ND5	chrM	1.361454	Down	0.000554983
MT-ND6	chrM	1.459269	Down	0.000966463
ARRDC3	chr5	1.278115	Up	0.003271461
SNORA33	chr6	1.966955	Up	0.000663895

Table 4. Genes applied for further evaluation

Gene name	Chromosome	Fold Change	Regulation Type	*P*-value	Network	Literature Review
ARRDC3	chr5	1.278115	Up	0.003271461	GI diseases	Tumor suppressor
CAV1	chr7	1.572301	Up	0	Cell cycle	Oncogene; tumor suppressor
DCBLD2	chr3	1.487044	Down	9.10E-14	Cellular movement	Oncogene; tumor suppressor
DCUN1D1	chr3	1.309115	Down	6.19E-05	Cancer	Oncogene
GADD45A	chr1	1.267846	Up	0.006050188	Cellular movement	Tumor suppressor
NES	chr1	1.321734	Down	0.00016649	Cellular movement	Oncogene

ARRDC3: arrestin domain containing 3; CAV1: caveolin 1; DCBLD2: discoidin, CUB and LCCL domain containing 2; DCUN1D1: defective in cullin neddylation 1 domain containing 1; GADD45A: growth arrest and DNA damage inducible alpha; NES: nestin.

was upregulated, while DCBLD2, DCUN1D1 and NES were downregulated in MKN45 cells with knockdown of EP2 receptor (**Figure 6A**). Similarly, gene expressions were also evaluated in paired primary gastric cancer tissues. Results indicated that CAV1 was downregulated in around 68.8% (22 out of 32) of the gastric cancer tissues. While NES was upregulated in around 34.4% (11 out of 32) of the gastric cancer tissues (**Figure 6B**). However, DCBLD2 and DCUN1D1 were downregulated in cancer tissues (Supplementary Figure 3). Taken together, it suggested that CAV1 was a potential downstream target of EP2 receptor in gastric cancer.

Discussion

Several studies reported that EP2 receptor expression was increased in various cancers including gastric cancer [15-17]. There is growing evidence antagonizing EP receptor could be a promising approach to suppress tumor growth and metastasis in various cancers [18, 19]. Evidence showed that PGE_2 mediated EGFR/MAPK signaling through the binding to EP2 receptor which stimulated cell growth and invasion [20, 21]. Studies showed that blocking EP2 receptor reduced the growth and invasion in prostate and colon cancer [22, 23]. In addition, dual administration of COX-2 and EP4 receptor antagonist significantly reduced tumor growth and metastasis in breast cancer model, through AKT phosphorylation [24]. Antagonism of EP receptors could be an alternative for cancer treatment by blocking the PGE_2/EP receptor signaling, however, little is known about the molecular mechanism of EP receptor in cancer.

To date, there is no chemotherapy combination that can treat locally advanced or metastatic gastric cancer. Results of a clinical trial reported that patients with resectable gastric tumors had improved progress-free and overall survival when they were given a preoperative ECF regimen [25]. In spite of the poor complete response, ECF regimen is still the standard treatment strategy to treat these patients [26]. Our data suggested that inhibition of EP2 receptor inhibit proliferation, enhanced apoptosis and sensitized gastric cancer cells to

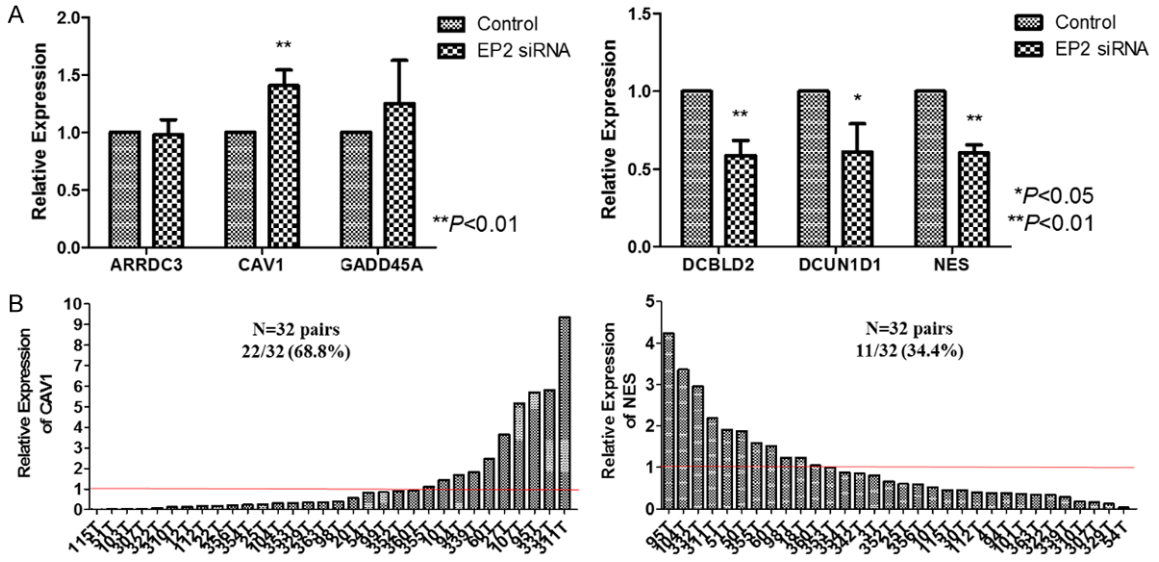

Figure 6. Expressions of six genes in gastric cancer cells and tissues. A. Expressions of six genes were evaluated in MKN45 cells with control or EP2 receptor siRNA. CAV1 was significantly upregulated, while DCBLD2, DCUN1D1 and NES were significantly downregulated (*P<0.05, **P<0.01). B. Expressions of CAV1 and NES were evaluated in paired gastric tumor and adjacent non-tumor tissues. CAV1 was downregulated in around 68.8% (22 out of 32) of the cancer tissues. NES was upregulated in around 34.4% (11 out of 32) of the cancer tissues. Relative expression represented the ratio of expression in tumor to non-tumor for each pair of tissues.

ECF. Many studies revealed that celecoxib enhanced cisplatin sensitivity in cancers [27, 28]. Similarly, inhibition of EP2 receptor increased cisplatin sensitivity through upregulation of ERβ in bladder cancer [29]. In bladder cancer, 3-methylcholanthrene inducing tumorigenesis through upregulation of EP2/EP4 receptor expressions were alleviated by EP2/EP4 receptor antagonist [30]. All these studies support the beneficial effect of EP2 receptor on chemodrug sensitivity in various tumors.

Effective drug delivery and drug accumulation in cells are factors to affect drug resistance. Several transporters and chaperones are crucial for homeostasis of copper to maintain a constant intracellular copper level and avoid copper toxicity. CTR1 is one of the important copper transporters that help to regulate copper homeostasis in the cells. It is a high affinity copper influx transporter allowing copper entering the cells in an energy-independent manner, and function as a transporter of platinum-containing chemotherapeutic drugs [31]. Cisplatin elicits the degradation of CTR1 to preclude drug uptake and accumulation inside the cells. Silencing of CTR1 increased the resistance to cisplatin *in vitro* and *in vivo* [32]. The efflux of cisplatin from cells is regulated by copper exporters, ATP7A and ATP7B. Recent findings demonstrated that targeting ATP7A improved the treatment response in neuroblastoma and pancreatic cancer [33, 34]. ATP7B has been shown to highly expressed in poorly differentiated than in well differentiated carcinoma, implicating ATP7B might be involved in chemoresistance against cisplatin in gastric cancer [35]. Similar findings were also shown in breast and ovarian carcinoma [36, 37]. Increased expressions of ATP7A and ATP7B decreased the sensitivity to cisplatin in cancer cell lines [38]. In this study, we also found that ATP7A and ATP7B expressions were upregulated upon ECF treatment, and were abrogated by EP2 receptor siRNA. These data suggest that EP2 receptor silencing enhanced the retention of ECF via downregulation of ATP7A and ATP7B expressions.

Studies showed that CAV1 has dual roles in the tumorigenesis of cancers, it acts as both tumor suppressor and oncogene [39, 40]. There are studies reporting the tumor suppressive role of CAV1 in tumorigenesis, knockdown of CAV1 expression increased invasion and incidence of lymph node metastasis in skin tumors [41]. Tumor hypoxia is a common feature in many solid tumors, hypoxia-induced HIF-1α trans-

criptional activity and nitric oxide synthase activity were alleviated by CAV1 overexpression and subsequently repressed tumor growth [42]. Conversely, CAV1 has reported to stimulate epithelial-mesenchymal transition progression and metastatic potential in hepatocellular carcinoma tumorigenesis [43, 44]. In gastric cancer, high WNT6 expression was correlated with tumor stage. Treatment with epirubicin and doxorubicin mediated the induction of WNT6/CAV1 expressions which increased the resistance to anthracycline drugs in gastric cancer cells [45]. In another study, expression of miR-6792-3p was increased in primary gastric cancer tissues and associated with tumor stage. Transfection with miR-6792-3p inhibitor reduced cell proliferation and invasion through upregulation of CAV1 in gastric cancer cells. In addition, CAV1 was found to be the downstream target of miR-6792-3p by luciferase reporter assay [46]. In this study, we reported for the first time that expression of CAV1 was upregulated upon EP2 receptor siRNA transfection. Silencing of EP2 receptor may abrogate cell proliferation and enhanced chemosensitivity to ECF through CAV1 upregulation.

Conclusion

In conclusion, our results illustrated that blocking EP2 receptor reduced tumorigenesis and induced apoptosis in gastric cancer. This study for the first time unravel EP2 receptor sensitized cancer cells to ECF in gastric cancer and CAV1 is a downstream target of EP2 receptor. Thus, EP2 receptor could be a potential therapeutic target in gastric tumors, in particular those with high EP2 receptor expression.

Disclosure of conflict of interest

None.

Address correspondence to: Drs. Kent-Man Chu and Vivian Yvonne Shin, Department of Surgery, The University of Hong Kong, Queen Mary Hospital, Pokfulam, Hong Kong 999077, China. Fax: +852 2819 4221; E-mail: chukm@hku.hk (KMC); vyshin@hku.hk (VYS)

References

[1] Bray F, Ferlay J, Soerjomataram I, Siegel RL, Torre LA and Jemal A. Global cancer statistics 2018: GLOBOCAN estimates of incidence and mortality worldwide for 36 cancers in 185 countries. CA Cancer J Clin 2018; 68: 394-424.

[2] Leung WK, Wu MS, Kakugawa Y, Kim JJ, Yeoh KG, Goh KL, Wu KC, Wu DC, Sollano J, Kachintorn U, Gotoda T, Lin JT, You WC, Ng EK and Sung JJ; Asia Pacific Working Group on Gastric Cancer. Screening for gastric cancer in Asia: current evidence and practice. Lancet Oncol 2008; 9: 279-87.

[3] Santoro A, Bufo P, Russo G, Cagiano S, Papagerakis S, Bucci P, Aquino G, Longo F, Feola A, Giordano A, Di Carlo A, Di Domenico M and Pannone G. Expression and clinical implication of cyclooxygenase-2 and E-cadherin in oral squamous cell carcinomas. Cancer Biol Ther 2020; 21: 667-674.

[4] Thiel A, Mrena J and Ristimäki A. Cyclooxygenase-2 and gastric cancer. Cancer Metastasis Rev 2011; 30: 387-95.

[5] Chan G, Boyle JO, Yang EK, Zhang F, Sacks PG, Shah JP, Edelstein D, Soslow RA, Koki AT, Woerner BM, Masferrer JL and Dannenberg AJ. Cyclooxygenase-2 expression is up-regulated in squamous cell carcinoma of the head and neck. Cancer Res 1999; 59: 991-4.

[6] Tong D, Liu Q, Wang LA, Xie Q, Pang J, Huang Y, Wang L, Liu G, Zhang D, Lan W and Jiang J. The roles of the COX2/PGE2/EP axis in therapeutic resistance. Cancer Metastasis Rev 2018; 37: 355-368.

[7] Lala PK, Nandi P and Majumder M. Roles of prostaglandins in tumor-associated lymphangiogenesis with special reference to breast cancer. Cancer Metastasis Rev 2018; 37: 369-384.

[8] Mizuno R, Kawada K and Sakai Y. Prostaglandin E2/EP signaling in the tumor microenvironment of colorectal cancer. Int J Mol Sci 2019; 20: 6254.

[9] Narumiya S, Sugimoto Y and Ushikubi F. Prostanoid receptors: structures, properties, and functions. Physiol Rev 1999; 79: 1193-226.

[10] O'Callaghan G and Houston A. Prostaglandin E2 and the EP receptors in malignancy: possible therapeutic targets? Br J Pharmacol 2015; 172: 5239-50.

[11] Ye Y, Wang X, Jeschke U and von Schönfeldt V. COX-2-PGE2-EPs in gynecological cancers. Arch Gynecol Obstet 2020; 301: 1365-1375.

[12] Woolbright BL, Pilbeam CC and Taylor JA 3rd. Prostaglandin E2 as a therapeutic target in bladder cancer: From basic science to clinical trials. Prostaglandins Other Lipid Mediat 2020; 148: 106409.

[13] Shin VY, Jin HC, Ng EK, Cho CH, Leung WK, Sung JJ and Chu KM. 4-(Methylnitrosamino)-1-(3-pyridyl)-1-butanone promoted gastric can-

cer growth through prostaglandin E receptor (EP2 and EP4) in vivo and in vitro, Cancer Sci 2011; 102: 926-33.
[14] Shin VY, Jin H, Ng EK, Cheng AS, Chong WW, Wong CY, Leung WK, Sung JJ and Chu KM. NF-kappaB targets miR-16 and miR-21 in gastric cancer: involvement of prostaglandin E receptors. Carcinogenesis 2011; 32: 240-5.
[15] Takehara H, Iwamoto J, Mizokami Y, Takahashi K, Ootubo T, Miura S, Narasaka T, Takeyama H, Omata T, Shimokobe K, Ito M and Matsuoka T Involvement of cyclooxygenase-2--prostaglandin E2 pathway in interleukin-8 production in gastric cancer cells. Dig Dis Sci 2006; 51: 2188-97.
[16] Cheuk IW, Shin VY, Siu MT, Tsang JY, Ho JC, Chen J, Tse GM, Wang X and Kwong A Association of EP2 receptor and SLC19A3 in regulating breast cancer metastasis. Am J Cancer Res 2015; 5: 3389-99.
[17] Lian S, Xia Y, Ung TT, Khoi PN, Yoon HJ, Lee SG, Kim KK and Jung YD. Prostaglandin E2 stimulates urokinase-type plasminogen activator receptor via EP2 receptor-dependent signaling pathways in human AGS gastric cancer cells. Mol Carcinog 2017; 56: 664-680.
[18] Watanabe Y, Imanishi Y, Ozawa H, Sakamoto K, Fujii R, Shigetomi S, Habu N, Otsuka K, Sato Y, Sekimizu M, Ito F, Ikari Y, Saito S, Kameyama K and Ogawa K. Selective EP2 and Cox-2 inhibition suppresses cell migration by reversing epithelial-to-mesenchymal transition and Cox-2 overexpression and E-cadherin downregulation are implicated in neck metastasis of hypopharyngeal cancer. Am J Transl Res 2020; 12: 1096-1113.
[19] Takahashi T, Uehara H, Ogawa H, Umemoto H, Bando Y and Izumi K. Inhibition of EP2/EP4 signaling abrogates IGF-1R-mediated cancer cell growth: involvement of protein kinase C-theta activation. Oncotarget 2015; 6: 4829-44.
[20] Sonoshita M, Takaku K, Sasaki N, Sugimoto Y, Ushikubi F, Narumiya S, Oshima M and Taketo MM. Acceleration of intestinal polyposis through prostaglandin receptor EP2 in Apc (Delta 716) knockout mice. Nat Med 2001; 7: 1048-51.
[21] Donnini S, Finetti F, Solito R, Terzuoli E, Sacchetti A, Morbidelli L, Patrignani P and Ziche M. EP2 prostanoid receptor promotes squamous cell carcinoma growth through epidermal growth factor receptor transactivation and iNOS and ERK1/2 pathways. FASEB J 2007; 21: 2418-30.
[22] Ma X, Aoki T, Tsuruyama T and Narumiya S. Definition of prostaglandin E2-EP2 signals in the colon tumor microenvironment that amplify inflammation and tumor growth. Cancer Res 2015; 75: 2822-32.
[23] Jiang J and Dingledine R. Role of prostaglandin receptor EP2 in the regulations of cancer cell proliferation, invasion, and inflammation. J Pharmacol Exp Ther 2013; 344: 360-7.
[24] Xin X, Majumder M, Girish GV, Mohindra V, Maruyama T and Lala PK. Targeting COX-2 and EP4 to control tumor growth, angiogenesis, lymphangiogenesis and metastasis to the lungs and lymph nodes in a breast cancer model. Lab Invest 2012; 92: 1115-28.
[25] Cunningham D, Allum WH, Stenning SP, Thompson JN, Van de Velde CJ, Nicolson M, Scarffe JH, Lofts FJ, Falk SJ, Iveson TJ, Smith DB, Langley RE, Verma M, Weeden S, Chua YJ; MAGIC Trial Participants. Perioperative chemotherapy versus surgery alone for resectable gastroesophageal cancer, N Engl J Med 2006; 355: 11-20.
[26] Van Cutsem E, Van de Velde C, Roth A, Lordick F, Köhne CH, Cascinu S and Aapro M; European Organisation for Research and Treatment of Cancer (EORTC)-gastrointestinal cancer group. Expert opinion on management of gastric and gastro-oesophageal junction adenocarcinoma on behalf of the European Organisation for Research and Treatment of Cancer (EORTC)-gastrointestinal cancer group. Eur J Cancer 2008; 44: 182-94.
[27] Xu HB, Shen FM and Lv QZ. Celecoxib enhanced the cytotoxic effect of cisplatin in chemo-resistant gastric cancer xenograft mouse models through a cyclooxygenase-2-dependent manner. Eur J Pharmacol 2016; 776: 1-8.
[28] Hashitani S, Urade M, Nishimura N, Maeda T, Takaoka K, Noguchi K and Sakurai K. Apoptosis induction and enhancement of cytotoxicity of anticancer drugs by celecoxib, a selective cyclooxygenase-2 inhibitor, in human head and neck carcinoma cell lines. Int J Oncol 2003; 23: 665-72.
[29] Goto T, Kashiwagi E, Jiang G, Nagata Y, Teramoto Y, Baras AS, Yamashita S, Ito A, Arai Y and Miyamoto H. Estrogen receptor-beta signaling induces cisplatin resistance in bladder cancer. Am J Cancer Res 2020; 10: 2523-2534.
[30] Kashiwagi E, Inoue S, Mizushima T, Chen J, Ide H, Kawahara T, Reis LO, Baras AS, Netto GJ and Miyamoto H. Prostaglandin receptors induce urothelial tumourigenesis as well as bladder cancer progression and cisplatin resistance presumably via modulating PTEN expression. Br J Cancer 2018; 118: 213-223.
[31] Larson CA, Blair BG, Safaei R and Howell SB. The role of the mammalian copper transporter 1 in the cellular accumulation of platinum-based drugs. Mol Pharmacol 2009; 75: 324-30.
[32] Ishida S, McCormick F, Smith-McCune K and Hanahan D. Enhancing tumor-specific uptake

of the anticancer drug cisplatin with a copper chelator. Cancer Cell 2010; 17: 574-83.
[33] Cheung BB and Marshall GM. Targeting ATP7A to increase the sensitivity of neuroblastoma cells to retinoid therapy. Curr Cancer Drug Targets 2011; 11: 826-36.
[34] Canu B, Fioravanti A, Orlandi P, Di Desidero T, Alì G, Fontanini G, Di Paolo A, Del Tacca M, Danesi R and Bocci G. Irinotecan synergistically enhances the antiproliferative and proapoptotic effects of axitinib in vitro and improves its anticancer activity in vivo. Neoplasia 2011; 13: 217-29.
[35] Ohbu M, Ogawa K, Konno S, Kanzaki A, Terada K, Sugiyama T and Takebayashi Y. Copper-transporting P-type adenosine triphosphatase (ATP7B) is expressed in human gastric carcinoma. Cancer Lett 2003; 189: 33-8.
[36] Kanzaki A, Toi M, Neamati N, Miyashita H, Oubu M, Nakayama K, Bando H, Ogawa K, Mutoh M, Mori S, Terada K, Sugiyama T, Fukumoto M and Takebayashi Y. Copper-transporting P-type adenosine triphosphatase (ATP7B) is expressed in human breast carcinoma. Jpn J Cancer Res 2002; 93: 70-7.
[37] Nakayama K, Kanzaki A, Ogawa K, Miyazaki K, Neamati N and Takebayashi Y. Copper-transporting P-type adenosine triphosphatase (ATP7B) as a cisplatin based chemoresistance marker in ovarian carcinoma: comparative analysis with expression of MDR1, MRP1, MRP2, LRP and BCRP. Int J Cancer 2002; 101: 488-95.
[38] Safaei R, Otani S, Larson BJ, Rasmussen ML and Howell SB. Transport of cisplatin by the copper efflux transporter ATP7B. Mol Pharmacol 2008; 73: 461-8.
[39] Ketteler J and Klein D. Caveolin-1, cancer and therapy resistance. Int J Cancer 2018; 143: 2092-2104.
[40] Williams TM and Lisanti MP. Caveolin-1 in oncogenic transformation, cancer, and metastasis. Am J Physiol Cell Physiol 2005; 288: C494-506.
[41] Trimmer C, Bonuccelli G, Katiyar S, Sotgia F, Pestell RG, Lisanti MP and Capozza F. Cav1 suppresses tumor growth and metastasis in a murine model of cutaneous SCC through modulation of MAPK/AP-1 activation. Am J Patho 2013; 182: 992-1004.
[42] Sanhueza C, Bennett JC, Valenzuela-Valderrama M, Contreras P, Lobos-González L, Campos A, Wehinger S, Lladser Á, Kiessling R, Leyton L and Quest AFG. Caveolin-1-Mediated tumor suppression is linked to reduced HIF1alpha S-Nitrosylation and transcriptional activity in hypoxia. Cancers (Basel) 2020; 12: 2349.
[43] Zhang C, Huang H, Zhang J, Wu Q, Chen X, Huang T, Li W, Liu Y and Zhang J. Caveolin-1 promotes invasion and metastasis by upregulating Pofut1 expression in mouse hepatocellular carcinoma, Cell Death Dis 2019; 10: 477.
[44] Yu H, Shen H, Zhang Y, Zhong F, Liu Y, Qin L and Yang P. CAV1 promotes HCC cell progression and metastasis through Wnt/beta-catenin pathway. PLoS One 2014; 9: e106451.
[45] Yuan G, Regel I, Lian F, Friedrich T, Hitkova I, Hofheinz RD, Ströbel P, Langer R, Keller G, Röcken C, Zimmermann W, Schmid RM, Ebert MP and Burgermeister E. WNT6 is a novel target gene of caveolin-1 promoting chemoresistance to epirubicin in human gastric cancer cells. Oncogene 2013; 32: 375-87.
[46] Luo Z, Rong Z, Zhang J, Zhu Z, Yu Z, Li T, Fu Z, Qiu Z and Huang C. Circular RNA circCCDC9 acts as a miR-6792-3p sponge to suppress the progression of gastric cancer through regulating CAV1 expression. Mol Cancer 2020; 19: 86.

Supplementary Table 1. Primers of genes for qPCR in this study

Gene Symbol	Primers
EP1	F 5'-TTGTCGGTATCATGGTGGT-3'
	R 5'-AGTAGGATGTACACCCAAGG-3'
EP2	F 5'-TTCTCCTGGCTATCATGACC-3'
	R 5'-AAGGATGGCAAAGACCCAAG-3'
EP3	F 5'-CAGCTTATGGGGATCATGTG-3'
	R 5'-ATCTGGTTCAGTGAAGCCAG-3'
EP4	F 5'-TCTTACTCATTGCCACCTCC-3'
	R 5'-GGTTCACAGAAGCAATTCGG-3'
ATB7A	F 5'-ATGATGAGCTGTGTGGCTTG-3'
	R 5'-TGCCAACCTGAGAAGCAATAG-3'
ATB7B	F 5'-TACCCATTGCAGCAGGTGTC-3'
	R 5'-ACTTGAGCTGCAGGGATGAG-3'
CTR1	F 5'-AGCTGGAGAAATGGCTGGAG-3'
	R 5'-AGGTGAGGAAAGCTCAGCATC-3'
Actin	F 5'-GCCAACACAGTGCTGTCTGG-3'
	R 5'-GCTCAGGAGGAGCAATGATCTTG-3'
ARRDC3	F 5'-GAGCAACAGCCCTCAACTCT-3'
	R 5'-CAGGTGAACGCATCACTTGC-3'
CAV1	F 5'-AATACGTAGACTCGGAGGGACA-3'
	R 5'-GCGGTAAAACCAGTATTTCGTC-3'
GADD45A	F 5'-TGAGTGAGTGCAGAAAGCAG-3'
	R 5'-TTTGCTGAGCACTTCCTCCA-3'
DCBLD2	F 5'-GGCCCTGAGAGTGGAACCCTTACAT-3'
	R 5'-TTCATTTGCAACCCCAGACCAC-3'
DCUN1D1	F 5'-ACTCGATCCAGCCAGCATTA-3'
	R 5'-TGTTTGGAGAACTCGCACTG-3'
NES	F 5'-TGGCAAAGGAGCCTACTCCAAGAA-3'
	R 5'-ATCGGGATTCAGCTGACTTAGCCT-3'
GAPDH	F 5'-TTGTTGCCATCAATGACCCC-3'
	R 5'-GCCTTCTCCATGGTGGTGAA-3'

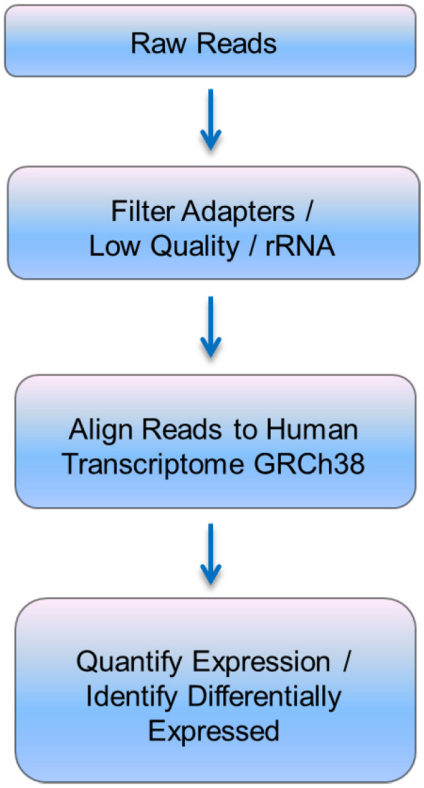

Supplementary Figure 1. Workflow of next generation sequencing. Sequencing raw reads were first filtered for adapter sequence and low quality sequence followed by retaining only reads with read length ≥40 bp. Subsequently, sequencing reads were filtered for rRNA sequence and remaining reads were used for downstream analysis. RSEM Version 1.2.21 was used for alignment to human transcriptome GRCh38, quantification of expression, and identification of differentially expressed genes. EBSeq Version 1.6.0 was used for the identification of differentially expressed genes.

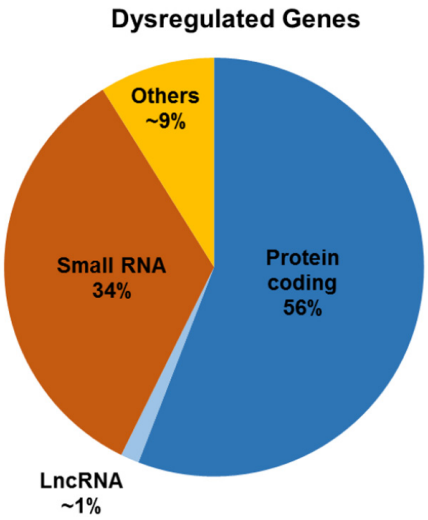

Supplementary Figure 2. Classification of downstream targets of EP2 from next generation sequencing. 281 genes with differential expressions were identified from expression profiles between MKN45-siControl and MKN45-siEP2. Percentage of the dysregulated genes were classified according to their types.

Supplementary Table 2. 281 genes with differential expressions from next generation sequencing

Gene name	chr	MKN45-Control TPM	MKN45-siRNA EP2 TPM	Real Fold Change	Regulation Type	*p*-value
EP2	chr14	11.52	5.81	1.771408	Down	9.99201E-16
protein coding						
CAV1	chr7	88.41	121.33	1.572301	Up	0
TMEM189-UBE2V1	chr20	1.04	2.88	3.173526	Up	0
CHURC1-FNTB	chr14	0.45	2.13	5.106366	Up	0
MPZL2	chr11	107.71	62.77	1.540662	Down	0
PLCXD1	chrX	2.1	4.83	10.0031	Up	0
RPL17-C18orf32	chr18	4.99	9.84	2.213617	Up	0
RP13-1032I1.10	chr17	0	1.38	13955.19	Up	0
PLCXD1	chrY	7.18	2.86	4.026666	Down	0
FAM156B	chrX	3.9	1.44	2.236707	Down	9.99201E-16
RP11-574F21.3	chr1	0.62	0.05	32.23745	Down	9.99201E-16
DCBLD2	chr3	25.12	16.46	1.487044	Down	9.10383E-14
KLHL42	chr12	18.66	12.62	1.454888	Down	1.18709E-11
FGL2	chr7	0.32	0.85	3.016978	Up	2.2997E-11
PTPRR	chr12	5.12	7.35	1.6791	Up	1.11768E-10
ATP11C	chrX	12.85	8.13	1.445964	Down	2.97136E-10
RP11-298I3.5	chr14	0	0.99	4203.513	Up	3.81081E-10
CTD-3074O7.11	chr11	0.26	0	4208.95	Down	7.62657E-10
SH3BGRL2	chr6	29.82	18.55	1.403358	Down	8.52653E-10
DENR	chr12	52	32.23	1.401552	Down	1.02759E-09
C1QTNF3-AMACR	chr5	0.25	0	3963.025	Down	3.94153E-09
UHMK1	chr1	30.56	19.46	1.374	Down	4.53414E-09
CTD-2116N17.1	chr15	15.52	23.46	1.665978	Up	7.51372E-09
FILIP1L	chr3	2.28	3.6	1.742815	Up	7.84244E-09
AP003419.11	chr11	0	1.03	3694.273	Up	1.25227E-08
PRSS23	chr11	44.65	51.53	1.369579	Up	2.10492E-08
CTD-2192J16.17	chr19	0.18	0	3702.519	Down	2.25107E-08
DKK1	chr10	210.95	249.21	1.352854	Up	2.97152E-08
MINOS1-NBL1	chr1	0	0.5	3488.52	Up	5.14903E-08
AC002398.9	chr19	0.62	2	3.729111	Up	7.63351E-08
PGM2L1	chr11	10.39	12.39	1.367704	Up	8.33418E-08
CA9	chr9	4.6	2.07	2.049336	Down	9.26079E-08
PABPC4	chr1	58.84	68.33	1.352475	Up	1.43451E-07
NDRG1	chr8	25.18	14.99	1.393695	Down	1.49842E-07
C4orf46	chr4	15.33	8.79	1.420432	Down	1.93527E-07
KRT6B	chr12	15.66	9.42	1.45122	Down	2.17196E-07
EIF3CL	chr16	3.29	4.57	1.594222	Up	3.03453E-07
APOOL	chrX	9.87	6.52	1.428749	Down	3.56659E-07
EMC2	chr8	28.74	17.46	1.445782	Down	3.76891E-07
RP11-544M22.13	chr1	15.78	19.6	1.410702	Up	4.80982E-07
ADIRF	chr10	80.83	49.18	1.425913	Down	5.51979E-07
PALM2-AKAP2	chr9	0	0.12	3022.488	Up	1.27385E-06
TSPAN12	chr7	73.79	49.33	1.33371	Down	1.37732E-06
PEG10	chr7	2.39	2.98	1.499595	Up	1.63577E-06
MGAT4B	chr5	86.01	58.48	1.326723	Down	3.08098E-06
RP11-1212A22.4	chr16	18.9	6.4	1.540933	Down	3.57832E-06
PPM1L	chr3	11.17	7.38	1.340014	Down	5.23365E-06
RP11-295P9.13	chr10	0.24	1.09	5.04499	Up	6.10983E-06

MT-ND4	chrM	29.78	18.64	1.393679	Down	6.76219E-06
NDFIP2	chr13	31.52	20.97	1.344407	Down	7.63108E-06
SPECC1L-ADORA2A	chr22	0.28	0.32	3.232037	Up	9.53148E-06
CPD	chr17	41.74	28.46	1.306877	Down	1.10048E-05
VEGFA	chr6	90.22	59.2	1.306139	Down	1.49408E-05
ZNF625-ZNF20	chr19	0.82	1.48	2.08085	Up	2.1613E-05
MGAT3	chr22	1.38	0.57	1.964225	Down	5.54522E-05
DCUN1D1	chr3	29.59	22.25	1.309115	Down	6.19234E-05
PTGS2	chr1	48.13	54.06	1.292206	Up	7.27612E-05
CXCL8	chr4	15.13	18.23	1.377794	Up	8.81301E-05
C5orf24	chr5	25.47	18.07	1.302092	Down	0.000129648
ERRFI1	chr1	120.01	132.98	1.280873	Up	0.00015116
NES	chr1	11.17	7.38	1.321734	Down	0.00016649
TNFRSF11B	chr8	45.99	31.08	1.308948	Down	0.000179227
DYNC1I1	chr7	1.46	2.19	1.715791	Up	0.00017995
MIB1	chr18	22.4	15.88	1.288926	Down	0.000186253
CAMK2N1	chr1	9.8	6.3	1.427454	Down	0.000212743
NPIPA2	chr16	0.29	1.08	4.609435	Up	0.000232556
MYO15B	chr17	12.22	7.92	1.375963	Down	0.000301814
PLAU	chr10	21.62	24.44	1.308931	Up	0.000383819
CYP4F3	chr19	3.46	1.94	1.53462	Down	0.00040895
TMEM265	chr16	0.86	0.09	8.0126	Down	0.000414804
GDPD5	chr11	7.96	4.59	1.424192	Down	0.000424984
PDZD3	chr11	10.33	5.09	1.474219	Down	0.000456127
CDKN1A	chr6	45.24	50.26	1.283959	Up	0.000476092
ZFP91-CNTF	chr11	0.27	0	2206.553	Down	0.000524437
MT-ND5	chrM	16.98	10.88	1.361454	Down	0.000554983
RP11-903H12.5	chr14	3.85	5.33	1.588343	Up	0.000667843
RNASE4	chr14	27.97	18.05	1.331077	Down	0.000743747
COL7A1	chr3	2.64	1.77	1.45531	Down	0.000769925
AADAC	chr3	5.29	7.57	1.493834	Up	0.000797486
RP11-178L8.4	chr16	0	0.43	2085.282	Up	0.000827947
CTD-2545G14.7	chr17	0.62	0	2137.538	Down	0.000835528
MAPK15	chr8	18.44	12.05	1.409684	Down	0.000925438
MT-ND6	chrM	30.03	17.92	1.459269	Down	0.000966463
SPOPL	chr2	16.74	10.75	1.293045	Down	0.001009421
ATP5H	chr17	265.25	281.93	1.263401	Up	0.001366595
KBTBD7	chr13	6.86	4.48	1.337771	Down	0.001693802
NCS1	chr9	9.79	7.08	1.323084	Down	0.001727821
NPIPB3	chr16	1.84	2.95	2.118369	Up	0.001761339
ALS2CL	chr3	7.1	4.67	1.339237	Down	0.002371807
TAF9B	chrX	9.77	6.16	1.356287	Down	0.002456702
RGS2	chr1	8.93	10.96	1.413661	Up	0.002608779
ARRDC3	chr5	15.9	16.91	1.278115	Up	0.003271461
ARL14	chr3	63.16	69.84	1.267646	Up	0.003339985
SERPINA3	chr14	0	0.23	1877.471	Up	0.003488631
BORCS7-ASMT	chr10	0.15	0	1910.082	Down	0.003875116
C8orf44-SGK3	chr8	0.18	0.21	6.979173	Up	0.004997503
GIPC2	chr1	15.55	10.59	1.281601	Down	0.005193539
ATF3	chr1	7.76	8.78	1.392668	Up	0.005333828
AS3MT	chr10	0.09	0.36	4.416151	Up	0.005746133
ZNF449	chrX	5.01	3.16	1.385031	Down	0.006036144

GADD45A	chr1	45.73	51.4	1.267846	Up	0.006050188
LRRC58	chr3	18.7	13.03	1.253228	Down	0.006302783
BTAF1	chr10	31.67	21.97	1.249291	Down	0.007073255
PLSCR4	chr3	3.55	1.91	1.639568	Down	0.007335432
RP11-162P23.2	chr12	1.85	0.51	3.150376	Down	0.008034059
GRAMD1B	chr11	3.75	2.36	1.369087	Down	0.008136494
ABC7-42404400C24.1	chr10	0	0.06	1752.99	Up	0.008237581
NRP1	chr10	23.8	25.55	1.255486	Up	0.008614815
HSD17B11	chr4	25.67	18.04	1.28861	Down	0.009203589
EPS8L3	chr1	15.74	11.28	1.331531	Down	0.009230782
ACTA2	chr10	7.39	8.38	1.417433	Up	0.009238232
RP11-215A19.2	chr4	0	0.49	1735.501	Up	0.00929129
STK26	chrX	50.66	36.56	1.247588	Down	0.010705784
SEMA3B	chr3	12.61	8.08	1.309351	Down	0.010904548
TRIM2	chr4	82.12	57.76	1.240246	Down	0.012051141
MBNL1	chr3	58.89	64.58	1.239449	Up	0.012824855
SARNP	chr12	52.37	34.56	1.277967	Down	0.013210508
RP13-582O9.6	chr8	0.21	0.49	2.701054	Up	0.013681304
MT-ATP6	chrM	42.71	28.23	1.318694	Down	0.014895175
SEC16B	chr1	2.51	1.39	1.512287	Down	0.018520145
AKAP2	chr9	0.77	0.26	1.898385	Down	0.018759159
EPS8	chr12	74.32	52.89	1.236839	Down	0.018873147
RAB9A	chrX	23.01	15.34	1.301629	Down	0.018992839
RP11-315D16.2	chr15	1.77	3.25	2.102383	Up	0.019526551
TGIF2-C20orf24	chr20	1.1	2.15	2.246027	Up	0.020559278
TNFRSF19	chr13	1.61	2.09	1.468251	Up	0.020728505
CDK17	chr12	11.51	13.54	1.275207	Up	0.021339366
STEAP3	chr2	16.87	11.5	1.260221	Down	0.021417099
CXADR	chr21	20.43	15.05	1.248194	Down	0.022167439
ERN2	chr16	28.65	18.69	1.254233	Down	0.022714656
RNASEK-C17orf49	chr17	0.07	0.45	5.41872	Up	0.023916103
IL31RA	chr5	1.46	2.01	1.602874	Up	0.024354936
MOGAT2	chr11	9.35	5.95	1.368467	Down	0.024525387
MAP7D1	chr1	14.04	9.96	1.277496	Down	0.024543636
PLXNA3	chrX	4.43	2.27	1.35409	Down	0.024596664
SLC7A7	chr14	16.62	11.42	1.291558	Down	0.025698983
TRIM39-RPP21	chr6	0	0.18	1577.071	Up	0.027418147
ENGASE	chr17	36.76	27.35	1.245014	Down	0.028776113
RP4-734P14.4	chr20	1.14	0.24	4.19504	Down	0.030328361
RNF152	chr18	2.08	1.23	1.369654	Down	0.031289262
RAB43	chr3	2.84	2.67	1.531594	Down	0.033554735
MT-CO3	chrM	511.69	362.92	1.229021	Down	0.03501837
NR1H3	chr11	26.35	18.58	1.285944	Down	0.035341401
TMEM64	chr8	17.24	12.32	1.252787	Down	0.036845155
SH3D21	chr1	6.82	4.18	1.381422	Down	0.038048478
PPT2-EGFL8	chr6	2.42	1.04	1.842355	Down	0.038893738
STRA6	chr15	3.57	2.11	1.50514	Down	0.039972182
ARHGEF40	chr14	12.69	8.78	1.252998	Down	0.040044574
SLC17A9	chr20	9.67	6.19	1.301822	Down	0.041674802
INPP5D	chr2	1.74	2.27	1.448233	Up	0.042075734
PRRG4	chr11	8.3	5.73	1.265189	Down	0.042177567
MT-CO1	chrM	593.32	420.97	1.229636	Down	0.043338134

RP11-561B11.2	chr14	2.46	1.48	1.449961	Down	0.044812029
BLOC1S5-TXNDC5	chr6	1.18	1.64	1.590263	Up	0.046365241
ROBO3	chr11	3.98	2.16	1.551153	Down	0.047263449
SMIM11B	chr21	9.64	12.08	1.414941	Up	0.048037116
ATHL1	chr11	7.6	5.08	1.317333	Down	0.048853252
MEGF6	chr1	13.31	9.34	1.254133	Down	0.049494599
lincRNA						
RNU11	chr1	50.93	88.74	2.02019	Up	8.8799E-11
RP11-465B22.8	chr1	7.8	3.71	1.832875	Down	3.31793E-06
AC129778.2	chr9	0.19	1.09	10.59573	Up	1.02481E-05
RP1-140K8.5	chr6	0.29	0.53	2.084538	Up	3.5854E-05
small RNA						
RNU5E-1	chr1	931.72	1503.17	1.872298	Up	0
RNU5A-1	chr15	299.21	453.06	1.757983	Up	0
SNORA73B	chr1	8120.48	11449.03	1.627245	Up	0
RNU5B-1	chr15	421.72	691.2	1.902865	Up	0
RNU4-1	chr12	2541.08	4651.65	2.120475	Up	0
SNORA74A	chr5	57.76	108.01	2.158831	Up	0
SNORD32A	chr19	0	38.07	9572.647	Up	0
RNU4-2	chr12	2313.85	4333.18	2.169278	Up	0
RNVU1-7	chr1	4213.66	6211.24	1.704775	Up	0
RNU1-28P	chr14	3015.54	4208.55	1.614041	Up	0
RNU1-27P	chr14	3015.54	4208.55	1.614041	Up	0
RNU1-1	chr1	3015.54	4208.55	1.614041	Up	0
RNVU1-18	chr1	3015.54	4208.55	1.614041	Up	0
SNORD15A	chr11	19.19	0	9419.071	Down	0
RNU1-2	chr1	3015.54	4208.55	1.614041	Up	0
RNU1-4	chr1	3015.54	4208.55	1.614041	Up	0
RNU1-3	chr1	3015.54	4208.55	1.614041	Up	0
SNORA40	chr11	0	31.96	14568.34	Up	0
SNORD17	chr20	212.05	303.24	1.648494	Up	0
RNU2-2P	chr11	3552.92	5703.57	1.853862	Up	0
SCARNA10	chr12	459.82	818.04	2.046622	Up	0
SCARNA6	chr2	73.15	127.22	2.003362	Up	0
SCARNA5	chr2	57.98	118.06	2.344782	Up	0
SNORD3A	chr17	9320.9	15400.8	1.861534	Up	0
U1	chr1	3015.54	4208.55	1.614041	Up	0
SNORA73A	chr1	11150.24	14351.56	1.485404	Up	0
SCARNA16	chr17	209.31	339.23	1.872045	Up	0
U1	KI270713.1	3015.54	4208.55	1.614041	Up	0
RNU12	chr22	29.49	73.04	2.866973	Up	0
SNORA61	chr1	11.5	46.71	4.70975	Up	0
SNORD60	chr16	0	23.12	5707.57	Up	1.29896E-14
U2	chr17	893.34	1139.91	1.473567	Up	1.69864E-14
U2	chr17	893.34	1139.91	1.473567	Up	1.69864E-14
U2	chr17	893.34	1139.91	1.473567	Up	1.69864E-14
RNU2-1	chr17	893.34	1139.91	1.473567	Up	1.69864E-14
U2	chr17	893.34	1139.91	1.473567	Up	1.69864E-14
U2	chr17	893.34	1139.91	1.473567	Up	1.69864E-14
U2	chr17	893.34	1139.91	1.473567	Up	1.69864E-14
U2	chr17	893.34	1139.91	1.473567	Up	1.69864E-14
U2	chr17	893.34	1139.91	1.473567	Up	1.69864E-14

U2	chr17	893.34	1139.91	1.473567	Up	1.69864E-14
U2	chr17	893.34	1139.91	1.473567	Up	1.69864E-14
SNORD15B	chr11	1942.33	2413.89	1.439041	Up	4.62963E-13
SNORA31	chr13	30.54	63.49	2.409127	Up	1.92601E-12
SNORA68	chr19	99.11	152.68	1.785583	Up	7.62901E-12
SNORA18	chr11	0	9.7	4718.925	Up	1.1229E-11
RNU5E-6P	chr1	24.82	56.74	2.654116	Up	8.3894E-11
SNORA62	chr3	57.58	92.33	1.855603	Up	2.16183E-10
SNORA27	chr13	2.79	17.59	7.302481	Up	2.16847E-10
SNORA67	chr17	36.06	66.56	2.138749	Up	4.09514E-10
SNORA57	chr11	124.96	174.8	1.619491	Up	7.09685E-10
SNORA44	chr1	28.28	55.38	2.269693	Up	3.20053E-09
SNORA22	chr7	346.51	434.77	1.454239	Up	9.73658E-09
SNORA79	chr14	276.17	345.19	1.447082	Up	4.73253E-08
SNORA63	chr3	1513.96	1772.24	1.356995	Up	6.53528E-08
SNORA9	chr7	39.26	66.99	1.977684	Up	9.08286E-08
SNORA38	chr6	32.22	57.77	2.078572	Up	1.27507E-07
SCARNA1	chr1	47.24	71.08	1.739797	Up	4.95985E-07
SNORA64	chr16	0	5.95	2956.647	Up	2.00572E-06
RNU11	chr1	6.94	0	2974.463	Down	2.97354E-06
SNORA74B	chr5	14.07	25.55	2.096647	Up	8.94979E-06
RNU6-1	chr15	42.01	70.67	1.954867	Up	1.30139E-05
RNU6-4P	chr3	42.01	70.67	1.954867	Up	1.30139E-05
RNU6-5P	chr2	42.01	70.67	1.954867	Up	1.30139E-05
RNU6-3P	chrX	42.01	70.67	1.954867	Up	1.30139E-05
RNU6-2	chr19	42.01	70.67	1.954867	Up	1.30139E-05
RNU6-9	chr19	42.01	70.67	1.954867	Up	1.30139E-05
RNU6-6P	chr10	42.01	70.67	1.954867	Up	1.30139E-05
SNORD22	chr11	0	5.83	2660.362	Up	1.55009E-05
SNORA8	chr11	1217.69	1379.18	1.312185	Up	1.586E-05
SNORA22	chr7	913.03	1039.55	1.31963	Up	1.86739E-05
RNU5F-1	chr1	16.76	35.07	2.428785	Up	3.29886E-05
SNORA31	chr13	33.25	54.54	1.901609	Up	3.53359E-05
SNORA12	chr10	107.77	138.53	1.488373	Up	5.14875E-05
SNORD97	chr11	355.15	414.18	1.350799	Up	5.71615E-05
RNU4ATAC	chr2	45.25	68.75	1.761986	Up	8.15071E-05
SNORA71B	chr20	24.33	40.87	1.899689	Up	9.05144E-05
SNORD10	chr17	311.02	359.21	1.337741	Up	0.000373777
SNORA48	chr17	435.2	495.34	1.319087	Up	0.000408221
RNU6-36P	chr12	0	6.02	2175.813	Up	0.000442353
SNORA43	chr9	744.21	829.98	1.292386	Up	0.000491761
SNORA33	chr6	23.44	39.76	1.966955	Up	0.000663895
AATBC	chr21	2.39	1.58	1.603488	Down	0.000724125
SNORA76C	chr17	7.72	18.25	2.741643	Up	0.001386305
SNORA70	chrX	78.06	101.17	1.501935	Up	0.00215542
RNU6-15P	chr10	6.38	0	1983.956	Down	0.002355092
SNORA71E	chr20	0.78	6.3	9.293348	Up	0.00289451
SNORA10	chr16	92.87	117.33	1.464344	Up	0.003043807
SNORA76A	chr16	14.3	25.91	2.099744	Up	0.008254793
SNORA24	chr4	157.31	183.5	1.352361	Up	0.020055836
SNORA23	chr11	29.23	39.89	1.576601	Up	0.024690265
SNORA17	chr9	34.45	49.2	1.655455	Up	0.02511969

SNORA16A	chr1	24.03	36.73	1.771182	Up	0.027422408
SNORA72	chr8	6.72	15.02	2.590596	Up	0.035860718
SNORA14B	chr1	10.33	19.7	2.208484	Up	0.035985133
RNU6ATAC	chr9	137.02	160.92	1.362108	Up	0.040074169
others						
Metazoa_SRP	chr14	355.25	514.4	1.666706	Up	0
RP1-59D14.9	chr17	0.01	8.8	1151.718	Up	0
RNY3	chr7	971.5	1274.53	1.525484	Up	3.9968E-15
RPPH1	chr14	576.06	724.28	1.442996	Up	8.50431E-14
RP11-572P18.1	chr10	2.49	0	5107.113	Down	1.93001E-12
RP11-118A1.2	chr13	5.73	0	5072.12	Down	2.43505E-12
RP11-294N21.2	chr18	5.72	0	5068.231	Down	2.499E-12
IKBKGP1	chrX	0	0.72	3984.386	Up	1.71049E-09
RN7SL1	chr14	68242.14	78876.29	1.330395	Up	4.25834E-06
ZBTB45P1	chr2	0.43	0	2819.909	Down	8.40706E-06
MT-TV	chrM	139.34	208.13	1.745086	Up	1.01902E-05
DLGAP1-AS2	chr18	12.01	14.43	1.380556	Up	5.11378E-05
RNY1	chr7	2002.4	2233	1.29509	Up	6.64266E-05
AC006011.4	chr2	2.95	0.32	8.137193	Down	9.84312E-05
COLCA1	chr11	11.72	7.9	1.303674	Down	0.000394855
FAM3C2	chrX	119.67	134.65	1.291226	Up	0.000414447
ZBTB45P2	chr2	0	0.27	2161.411	Up	0.000488738
PKD1P1	chr16	6.48	4.34	1.304494	Down	0.003226667
PSMC1P1	chr3	10.16	12.3	1.387508	Up	0.004685774
RP11-267M23.1	chr8	6.94	4.32	1.403555	Down	0.009566646
CSPG4P10	chr15	0.25	0.06	3.745627	Down	0.015847663
Metazoa_SRP	chr14	61279.25	67136.27	1.26102	Up	0.019648287
BZW1P2	chr3	36.91	41.1	1.277542	Up	0.040993796
RP11-195O1.5	chr10	0.58	0	1537.791	Down	0.046145405

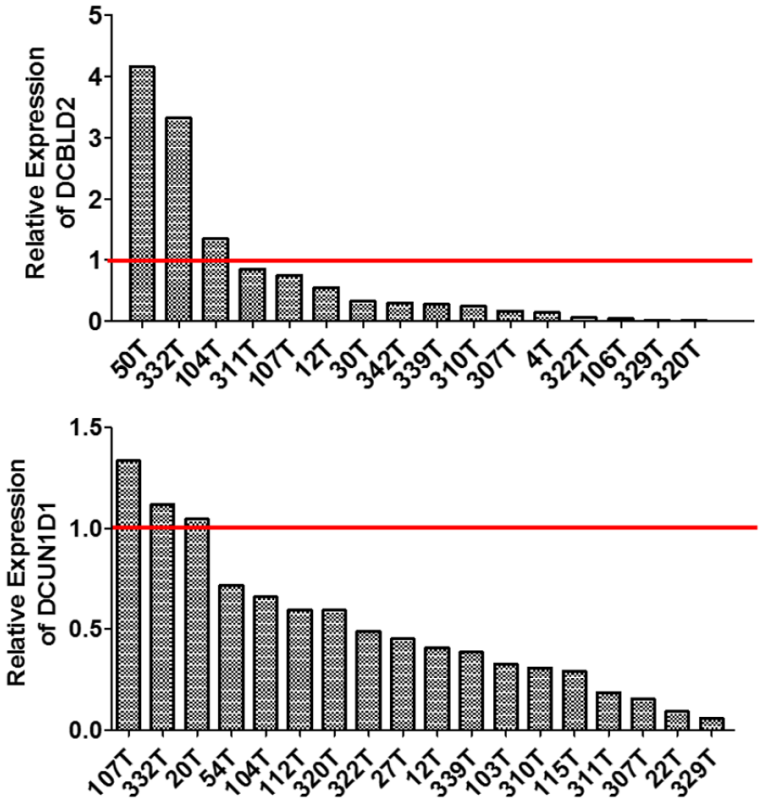

Supplementary Figure 3. Expressions of genes in gastric cancer tissue samples. Expressions of DCBLD2 and DCUN1D1 were evaluated in paired gastric tumor and adjacent non-tumor tissue samples. DCBLD2 was downregulated in around 80% (13 out of 16) of the cancer tissue samples. DCUN1D1 was downregulated in around 80% (15 out of 18) of the cancer tissue samples.